Investigation of the Reaction ^{4}He(^{4}He, ^{4}He)^{4}He* at 64 MeV†

E. E. Gross, E. V. Hungerford, III, and J. J. Malanify
Oak Ridge National Laboratory, Oak Ridge, Tennessee 37830
AND
H. G. Pugh and J. W. Watson
University of Maryland, College Park, Maryland 20740

(Received 7 October 1968)

The reaction ^{4}He(^{4}He, ^{4}He)^{4}He* was investigated, using a 64-MeV α-particle beam. Absolute differential cross sections for the state near 20-MeV excitation are reported for the angular range $12.5° < \theta_{c.m.} < 74°$. We measure the excitation energy of this state to be 20.28±0.05 MeV and the width to be 0.41±0.05 MeV. The shape and position of this state are shown to be consistent with an analysis based on the known properties of low-energy p-^{3}H scattering.

I. INTRODUCTION

In the last several years, the study of the $A=4$ system has been of special interest. Excited states of ^{4}He have been discovered in several nuclear reactions, while phase-shift analyses of n-^{3}H and p-^{3}He scattering have given information on the analog states in ^{4}H and ^{4}Li. All the states observed are particle-unstable and broad, which makes the interpretation of the data difficult and ambiguous.

The experimental picture of the excited states of ^{4}He is far from complete. The review article by Meyerhof and Tombrello[1] summarizes the present situation. Figure 1 shows a typical level scheme for ^{4}He. This was determined by Werntz and Meyerhof[2] from an R-matrix analysis of data from the reaction ^{3}H(p, n)^{3}He. In their analysis, they restricted the possible states to those which would be expected from shell-model considerations. From a shell-model viewpoint the odd-parity excited states of Fig. 1 are predominantly single-particle, single-hole states while the even-parity excited states are predominantly two-particle, two-hole states.

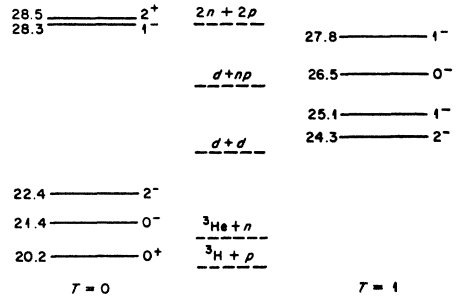

FIG. 1. Level diagram for excited states of ^{4}He. The values are taken from an R-matrix analysis (Ref. 2) of the data from the reaction ^{3}H(p, n)^{3}He. The energies at which the various breakup thresholds occur are indicated by the dashed lines.

In order to obtain further information on the excited states of ^{4}He we have studied inelastic α-particle scattering from ^{4}He. Of the levels shown in Fig. 1, the $T=1$ levels cannot be formed in this reaction if charge independence of nuclear forces is applicable, while the 0^- level cannot be formed if angular momentum and parity are conserved. Thus, the reaction is quite selective; in the present experiment we obtain information mainly on the 0^+ level near 20 MeV.

The 0^+ level was the first excited state of ^{4}He to be discovered and has been observed in a large variety of reactions,[3–10] but the various measurements of its excitation energy and width are not consistent. For example, in the ^{4}He(p, p')^{4}He* reaction the excitation energy and width were reported[7] as 20.46±0.14 and 0.34±0.04 MeV, respectively, while p-t coincidence spectra from the ^{3}H(d, pt)^{1}H reaction yielded[5] the values 19.94±0.02 and 0.140±0.025 MeV. It may well be that the energy and width of such a broad peak depend on the reaction used to study it.[11] We have made a special effort to determine the energy and width of this state as observed by inelastic α-particle scattering.

The experiment was performed with a 64-MeV beam, permitting study of states in ^{4}He up to 32-MeV excitation. A ΔE-E counter telescope was used to measure the energy spectrum of inelastically scattered α particles

† Research sponsored by the U.S. Atomic Energy Commission under contract with Union Carbide Corp.

[1] W. E. Meyerhof and T. A. Tombrello, Nucl. Phys. **A109**, 1 (1968). This reference includes an extensive bibliography for the $A=4$ nuclei.

[2] C. Werntz and W. E. Meyerhof, Nucl. Phys. **A121**, 38 (1968).

[3] H. W. Lefevre, R. R. Borchers, and C. H. Poppe, Phys. Rev. **128**, 1328 (1962); C. H. Poppe, Phys. Letters **2**, 171 (1962); C. H. Poppe, C. H. Holbrow, and R. R. Borchers, Phys. Rev. **129**, 733 (1963).

[4] P. G. Young and G. G. Ohlsen, Phys. Letters **8**, 124 (1964); **11**, 192 (1964).

[5] P. D. Parker, P. F. Donovan, J. V. Kane, and J. F. Mollenauer, Phys. Rev. Letters **14**, 15 (1965).

[6] J. Cerny, C. Détraz, and R. H. Pehl, Phys. Rev. Letters **15**, 300 (1965).

[7] L. E. Williams, Phys. Rev. **144**, 815 (1966).

[8] R. F. Frosch, R. E. Rand, H. Crannell, J. S. McCarthy, L. R. Suelzle, and M. R. Yearian, Nucl. Phys. **A110**, 657 (1968).

[9] N. Jarmie, R. H. Stokes, G. G. Ohlsen, and R. W. Newsome, Jr., Phys. Rev. **161**, 1050 (1967).

[10] E. L. Haase, H. Brückmann, W. Kluge, and L. Schänzler, in Proceedings of the Symposium on Light Nuclei, Few Body Problems and Nuclear Forces, Brela, Yugoslavia, 1967 (to be published).

[11] E. H. Berkowitz, Nucl. Phys. **60**, 555 (1964); E. Norbeck and F. D. Ingram, Phys. Rev. Letters **20**, 1178 (1968).

TABLE I. Contributions to the energy resolution for the reaction ^{4}He(^{4}He, ^{4}He)^{4}He* (20.3 MeV), in keV (FWHM).

Source of energy spread	Solid-state detector $\theta_{lab}=5°$	Solid-state detector $\theta_{lab}=15°$	Magnetic spectrograph $\theta_{lab}=5°$	Magnetic spectrograph $\theta_{lab}=13°$
Energy spread of beam	35	35	70	70
Energy straggling in foil	30	30	140	140
Energy straggling in gas	50	50	80	80
Detector resolution	125	125	45	45
Angular spread of beam	30	80	80	190
Small-angle scattering in foil	30	80	80	190
Small-angle scattering in gas	50	130	40	100
Angular acceptance of detector slits	90	240	70	170
Over-all resolution (lab)	180	330	220	380
Over-all resolution (c.m.)	135	240	165	280

and to construct an angular distribution for production of the 0^+ state. In addition, energy spectra were obtained at 5° and 13° with the broad-range magnetic spectrograph at ORIC.[12] This allowed a more precise determination of the energy of the 0^+ state.

II. EXPERIMENTAL METHOD

A. Solid-State-Detector Measurements

For this part of the experiment, an α-particle beam was extracted from ORIC, energy-analyzed, collimated to reduce the angular divergence, and focused at the center of a 76-cm-diam scattering chamber. The energy of the analyzed beam was 64.0±0.4 MeV and its calculated energy spread was 35 keV full width at half-maximum (FWHM). At the center of the scattering chamber the beam was 1.1 mm wide and 3.5 mm high with angular divergences of 0.14° FWHM horizontally and 0.20° FWHM vertically. The beam intensity was about 25 nA.

The gas target was provided by filling the entire scattering chamber with ^{4}He gas at a pressure of 20 cm Hg. The beam entered the gas through a 0.63-μ nickel foil 25 cm from the center of the chamber. The solid-state detectors were in the gas at a distance of 32 cm from the target volume with no windows in between. The slits defining target volume and solid angle were (a) 1.6 mm wide and 8.4 mm from the target and (b) 1.6 mm wide, 5.6 mm high, and 31 cm from the target.

The particles were detected in a ΔE-E system, consisting of a 0.10-mm totally depleted Si surface-barrier detector and a 1.5-mm partially depleted Si surface-barrier detector. The ΔE and $E+\Delta E$ signals were fed into a fast-pulse multiplier. The multiplier output and $E+\Delta E$ signal were displayed on a 20 000-channel pulse-height analyzer operating in a 20×1000 mode. No difficulties were encountered in distinguishing ^{4}He from other particles.

The effective energy resolution of the system is determined by several factors, the most important of which is, except at the smallest angles, the kinematical energy spread due to the finite angular resolution. The calculated contributions to the energy resolution for the 20-MeV state are given in Table I for $\theta_{lab}=5°$ and $\theta_{lab}=15°$. A similar calculation gave a good description of the shape of the elastic scattering peak.

Measurements were made at values of θ_{lab} between 5° and 27°, corresponding to c.m. angles between 12.5° and 74°. The measurements at various angles were normalized to each other by means of a Faraday cup and current integrator, and the absolute scale was obtained by normalizing the elastic scattering angular distribution to the 63.9±0.2-MeV data of Darriulat *et al.*[13] After correction for energy losses in the entrance foil and gas, the beam energy in the present experiment was 63.8±0.4 MeV. The agreement in shape of our elastic scattering angular distribution with that of Ref. 13 is very good, and we believe our absolute cross sections are accurate to better than 10%.

B. Magnetic Spectrograph Measurements

The broad-range magnetic spectrograph facility has been described elsewhere.[12] Basically, the spectrograph magnet is similar to the magnet described by Borggreen, Elbek, and Nielsen,[14] but scaled up to ORIC energies. For this experiment the scattering chamber contained ^{4}He gas at a pressure of 38 cm Hg, with 2.4-μ Havar entrance and exit windows. The acceptance angle of the spectrograph was limited to ±0.1° by a set of slits. By a series of calibrations to be described below, the

[12] J. B. Ball, IEEE Trans. Nucl. Sci. **NS13**, 340 (1966).

[13] P. Darriulat, G. Igo, H. G. Pugh, and H. D Holmgren, Phys. Rev. **137**, B315 (1965).

[14] J. Borggreen, B. Elbek, and L. P. Nielsen, Nucl. Instr. Methods **24**, 1 (1963).

TABLE II. Reactions used to calibrate the magnetic spectrograph.

Reaction	Lab angle of observation (deg)	Observed focal plane position (cm)	Energy by magnetic rigidity (MeV)	Energy by kinematics (MeV)
^{4}He(^{4}He, ^{4}He)^{4}He	35	110.66	42.64	42.64
^{4}He(^{4}He, ^{4}He)^{4}He	37	103.99	40.52	40.49
^{4}He(^{4}He, ^{4}He)^{4}He	39	96.95	38.33	38.31
^{4}He(^{4}He, ^{4}He)^{4}He	41	89.43	36.06	36.08
^{12}C(^{4}He, ^{4}He)^{12}C	69	106.26	41.23	41.18
^{4}He(^{4}He, ^{4}He)^{4}He*(20.3)	5	103.53	40.38	
^{4}He(^{4}He, ^{4}He)^{4}He*(20.3)	13	94.20	37.49	

beam energy at the center of the scattering chamber was determined to be 64.12±0.06 MeV.

The energy resolution of the system was calculated by combining the energy spread of the beam, energy straggling in passing through the gas and foils, and the kinematic spread. The various contributions are listed in Table I. Measurements on the incident beam made with and without gas and foils in place confirmed the energy spread and straggling calculations and also gave an accurate measurement of the energy lost by the particles in passing through the system.

In order to obtain an accurate value for the energy of the 20-MeV state of ^{4}He considerable care was taken to obtain absolute measurements of the incident and scattered energies. The angles of observation for the ^{4}He(^{4}He, ^{4}He)^{4}He* measurements were $\theta_{lab}=5°$ and $\theta_{lab}=13°$, chosen to be near maxima of the angular distribution as determined from the counter telescope data. To eliminate hysteresis effects in Fe, one field setting was used for both measurements and for all the calibrations. The calibrations were made by placing known particle groups near the position on the focal plane at which the 20-MeV state in ^{4}He was expected. Table II shows the reactions and scattering angles used for the calibration. A self-consistent analysis of these calibration lines gave the beam energy at the center of the scattering chamber as 64.12±0.06 MeV. Columns 4 and 5 of Table II show the good agreement achieved between determinations of the scattered-particle energies from the geometric properties of the spectrograph and from kinematic calculations which included small corrections for energy losses in foil and gas. The inelastic scattering groups corresponding to the 20-MeV state of ^{4}He are also given in Table II for comparison.

III. RESULTS

Figure 2 shows some of the α-particle spectra observed with the solid-state detectors. Each spectrum consists of a continuum of events superimposed upon an instrumental background. A peak observed at the high-energy end of the continuum at laboratory angles of 5° and 13° but not 19° corresponds to the first excited state of ^{4}He at about 20 MeV. In addition to this state, we see some evidence for structure near 26-MeV excitation but we have not made a detailed analysis of this structure. It should be pointed out that the reaction ^{4}He(^{4}He, ^{4}He)^{4}He* may proceed through the ground states of ^{5}Li and ^{5}He to produce α particles in this energy range, corresponding to an excitation energy of ^{4}He greater than 22 MeV. Our investigation has been mainly of the region near the 20-MeV state.

Figure 3 shows in more detail the spectrum near 20-MeV excitation for angles of $\theta_{lab}=5°$, 10°, and 15°. The lines drawn through the points have no theoretical significance; they were only used to estimate the cross section and width of the state. As shown in the figure, we have assumed the spectra to be composed of three parts: a constant background, a continuum, and a peak. After removal of the energy resolution we obtain for the peak a width of 0.41±0.05 MeV FWHM. The energy calibration for the solid-state-detector measurements was not reliable enough to quote an accurate value for the excitation energy of the state: This is obtained much more accurately from the spectrograph measurements.

Figure 4 shows the differential cross section for the peak, in the c.m. system, together with the elastic scattering for comparison. Note that the relationship between θ_{lab} and $\theta_{c.m.}$ is very different for the elastic and inelastic scattering.

Figures 5 and 6 show the magnetic spectrograph results. A constant background has been subtracted from the data by drawing a horizontal line through the data below the threshold for α-particle breakup. This background was 85% of the peak height at 5° but only 30% at 13°. The errors shown are due to statistics only, and only a relative cross-section scale is given. During scanning of the emulsion plates, tracks could be discriminated by direction but grain density considerations could not eliminate contamination of the spectra by ^{3}He, tritons, and deuterons. The energy spectra of these particles are expected to be smooth in this region

and are the probable source of the constant background which extends below the threshold for α-particle breakup.

As a result of the calibration procedure described in Sec. II, the energy of the 20-MeV state was determined to be 20.28±0.05 MeV, defined by the part of the peak with the highest cross section. The width of the peak after extraction of experimental resolution was found to be 0.4±0.1 MeV in the c.m. system, consistent with the value of 0.41±0.05 MeV determined from the solid-state-detector measurements. The spectra of Figs. 5 and 6 are consistent within statistics with the equivalent solid-state-detector spectra.

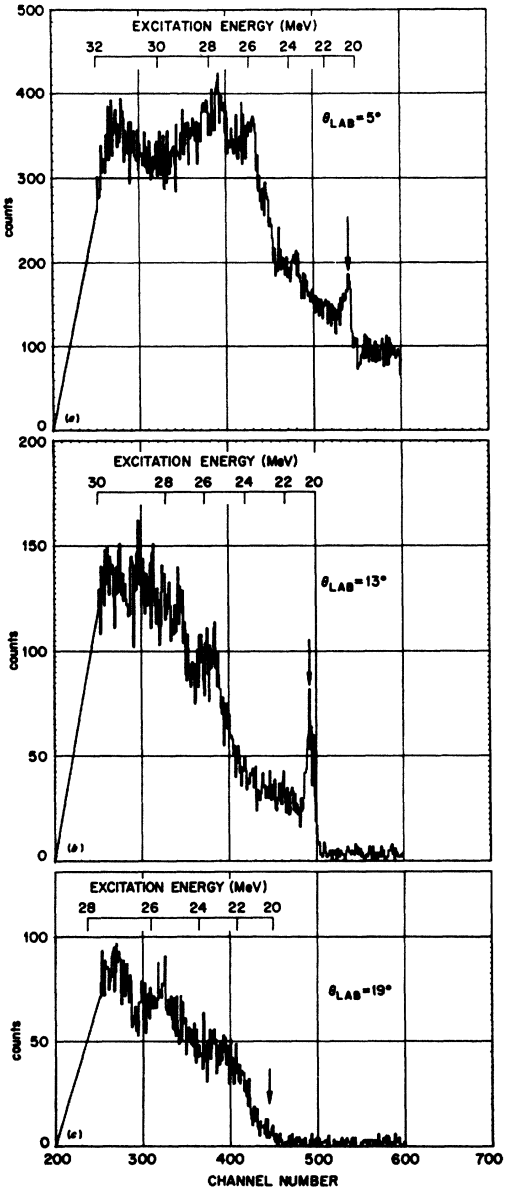

FIG. 2. α spectra from the reaction ^{4}He(^{4}He, ^{4}He)^{4}He* at 64 MeV obtained with the solid-state detector. The elastic scattering peak would be off the scale to the right and is not shown. The peak, indicated by the arrow, near the high-energy end of the continuum is due to the first excited state of ^{4}He near 20-MeV excitation.

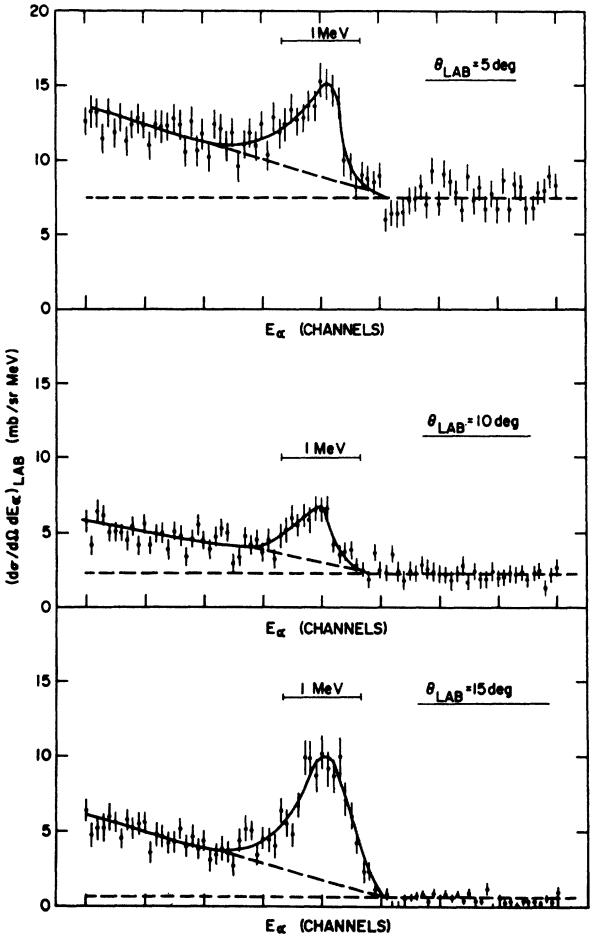

FIG. 3. α-particle spectra corresponding to excitation of the 20-MeV state in ^{4}He obtained with the solid-state detector. The lines are used to estimate the cross section and width of the state as discussed in the text.

IV. DISCUSSION

The excited state of ^{4}He observed most strongly in the present experiment is the state at 20.28±0.05 MeV, its width being 0.41±0.05 MeV. We assume this to be the 0^+, $T=0$ state observed by previous workers. For the higher states there is no clear evidence, though there are indications that more detailed study of the region of excitation near 26 MeV might be interesting. A comparison of the spectra from three inelastic scattering reactions shows systematic differences. Inelastic proton scattering[7] produced the 0^+ state but also the 2^-, $T=0$ state at about 22.4 MeV, which is weakly produced, if at all, by inelastic α or inelastic electron[8] scattering. This relative weakness of the excitation of an unnatural parity state is consistent with the systematics of inelastic α scattering from other nuclides.

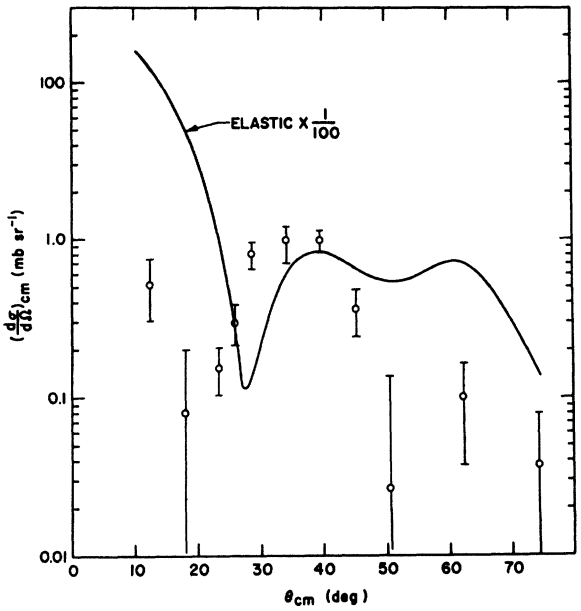

FIG. 4. Angular distribution for ^{4}He(^{4}He, ^{4}He)^{4}He* (20.3 MeV) at 64 MeV. For comparison, the solid curve is the angular distribution for elastic scattering.

The remainder of this discussion will be concerned with an analysis of our data on the 20.28-MeV state. The angular distribution (Fig. 4) for this state shows a diffractionlike behavior. We have not performed a sophisticated analysis of the angular distribution but have restricted ourselves to the simplest models. The simplest models are the plane-wave Born approximation (PWBA) with a zero-range interaction at the nuclear surface, and the sharp-cutoff Blair model of diffraction scattering.[15] In neither model is the angular-momentum transfer uniquely determined by the data. This is because of the large value of momentum transfer

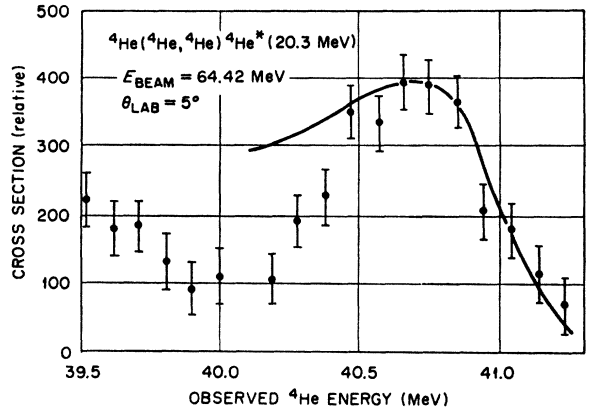

FIG. 5. α spectrum for the reaction ^{4}He(^{4}He, ^{4}He)^{4}He* (20.3 MeV) obtained with the magnetic spectrograph at $\theta_{lab}=5°$. The curve is the result of the final-state interaction calculation described in the text.

[15] J. S. Blair, Phys. Rev. 115, 928 (1959).

even at $\theta_{c.m.}=0$. If we assume $J=0^+$ for the 20.28-MeV state, we find that the Blair formula is somewhat more satisfactory than the PWBA, but in either case the fit is satisfactory only if we choose a very large interaction radius (e.g., 6.6 F) and identify the maximum at $\theta_{c.m.}=35°$ with the *second* subsidiary maximum predicted by the theory. In view of the enormous inelasticity of the process, the simple formulas would be suspect even if other conditions favored their application. In this connection it may be worth noting that in the *laboratory* system the maximum of the inelastic angular distribution coincides with the minimum of the elastic angular distribution.

We have analyzed the shape of the energy spectrum following the procedure of Yu and Meyerhof.[16] In these calculations the PWBA method is used and the excited states of ^{4}He are introduced as final-state interactions between the breakup particles. In the case of the

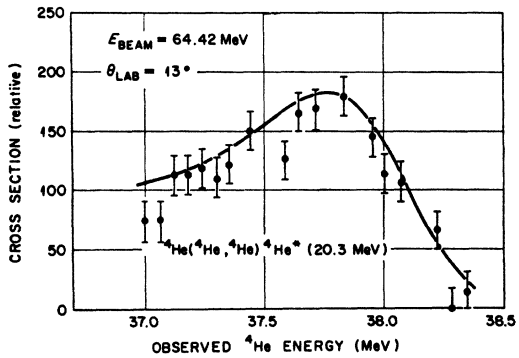

FIG. 6. α spectra for the reaction ^{4}He(^{4}He, ^{4}He)^{4}He* (20.3 MeV) obtained with the magnetic spectrograph at $\theta_{lab}=13°$. The curve is the result of the final-state interaction calculation described in the text.

20.28-MeV state the energy spectra of the inelastically scattered α particles are assumed to be dominated (below the threshold for n-^{3}He breakup) by the singlet S-wave phase shift for p-^{3}H scattering. The triplet phase shift is nonresonant and presumed to be unimportant.

The general features of such a calculation are set forth in detail in Ref. 17. For this particular case one assumes that the incident channel wave function is represented by a product of two α-particle wave functions, properly symmetrized, and a plane wave describing their c.m. motion. One then assumes that the exit channel is represented by a product of an α-particle ground-state wave function, an α-particle excited-state wave function, and a plane wave describing their c.m. motion. We take a Gaussian form for the α-particle ground-state wave function, $\psi_{^4He}$. The wave function for the first excited state, $\psi_{^4He^*}$, is approximated by a product of a wave function describing the c.m. motion

[16] D. U. L. Yu and W. E. Meyerhof, Nucl. Phys. 80, 481 (1966).
[17] B. J. Morton, E. E. Gross, E. V. Hungerford, J. J. Malanify, and A. Zucker, Phys. Rev. 169, 825 (1968).

TABLE III. Excitation energy and width of the 20.3-MeV state of ^{4}He as observed in several reactions.

Reaction	Ref.	Excitation energy (MeV)	Width (MeV)
^{3}H(d, n)^{4}He	3	20.1	0.3–0.4
^{3}He(d, p)^{4}He	9	20.08±0.04	0.43±0.05
^{3}He(t, d)^{4}He	9	20.00±0.04	0.36±0.05
^{3}He(d, pt)^{1}H	5	19.94±0.02	0.140±0.025
^{6}Li(p, ^{3}He)^{4}He ^{7}Li(p, ^{4}He)^{4}He	6	20.10±0.15	...
^{4}He(p, p')^{4}He	7	20.46±0.14	0.34±0.04
^{4}He(e, e')^{4}He	8	20.26±0.16	0.39±0.10
^{4}He(α, α')^{4}He	This work	20.28±0.05	0.41±0.05

of a singlet unbound proton and triton, φ_p, and a Gaussian wave function for the internal system of the triton, φ_t:

$$\psi_{^4\mathrm{He}} \propto \exp(-\tfrac{1}{2}\gamma^2 \sum_{i\neq j}^{4} |\, \mathbf{r}_i - \mathbf{r}_j \,|^2), \tag{1}$$

$$\psi_{^4\mathrm{He}^*} = \varphi_t \varphi_p, \tag{2}$$

$$\varphi_p \sim (G_0 \sin\delta + F_0 \cos\delta)/kr, \tag{3}$$

$$\varphi_t \propto \exp(-\tfrac{1}{2}\beta^2 \sum_{i\neq j}^{3} |\, \mathbf{r}_i - \mathbf{r}_j \,|^2). \tag{4}$$

Here δ is the singlet s-wave p-^{3}H elastic scattering phase shift, $F_0(G_0)$ is the regular (irregular) Coulomb wave function, and k is the relative p-^{3}H momentum. The interaction potential was assumed to be of a Gaussian form with a range parameter of 0.6 F^{-1}, and the α-particle range parameter γ and the triton range parameter β were both taken to be 0.4 F^{-1}.

The results of the calculation, with the experimental resolution folded in, are compared with the data in Figs. 5 and 6. The theoretical curves are quite insensitive to the α-particle and triton range parameters, provided that reasonable values are used. The shape of the spectrum is essentially determined by the singlet S-wave p-^{3}H phase shift, provided that we consider relative energies of the p-^{3}H system below about 1 MeV. Above 1 MeV, other phase shifts become increasingly important. The singlet S-wave phase shift was taken from Ref. 18. For each spectrum the theoretical curve was normalized to the data at the peak, but no shift of the energy scale was made.

This simple calculation gives an excellent prediction of the position of the peak at both 5° and 13°. The predicted shape of the peak agrees with the data within statistical accuracy at 13°, but the agreement is not as good at 5°. Experience in other reactions indicates that final-state interaction calculations are not equally successful at all angles of detection. In this case, however, we are inclined to mistrust the 5° spectrograph data insofar as the detailed shape of the peak is concerned, because a very large background subtraction had to be made. To confirm this we examined the solid-state-detector results at the same angles. At 13° the two sets of data are completely consistent if a small shift of the solid-state-detector spectrum is made to allow for the poor determination of its energy calibration. At 5°, however, the solid-state-detector results are in much better agreement with the shape predicted by the calculation. Since the background subtraction at 5° is much less for the solid-state-detector results, it seems reasonable to prefer this data for information on the shape of the peak and to conclude that the calculations are in agreement with experiment at both angles.

Finally, we compare our values for the excitation energy and width of the state with those obtained from other reactions. The various results are collected in Table III. We note that the results for both the energy and the width from the three inelastic scattering experiments are in agreement. The energies given by inelastic scattering seem to be about 0.2 to 0.3 MeV higher than in the other reactions. The widths from all the reactions except ^{3}He(d, pt)^{1}H agree within experimental uncertainties.

The success of the final-state interaction calculation indicates that the state that we observe at 20.28 MeV corresponds to almost a pure ^1S-wave resonance in the p-^{3}H system[19] and is consistent with a 0^+ assignment for this state. On the other hand, Yu and Meyerhof[16] found it necessary to include various amounts of ^1S, ^3S, ^1P, and ^3P waves in order to account for the location of the p-^{3}H peak produced in the ^{3}H(d, n)^{4}He* (20.1 MeV)[3] and ^{3}He(d, p)^{4}He* (20.08 MeV)[4] reaction data. Thus, the observed excitation energies of Table III may not

[18] W. E. Meyerhof and J. N. McElearney, Nucl. Phys. **74**, 533 (1965).

[19] C. Werntz, Phys. Rev. **128**, 1336 (1962); **133**, B19 (1963).

be in disagreement but the differences may be a manifestation of differing amounts of ^1S, ^3S, ^1P, and ^3P waves in the final-state p-^{3}H system.

These results are consistent with a simple model in which the relative strength of the various configurations in the final-state p-^{3}H system is dependent on the initial-state origin of the proton and triton. In the case of inelastic scattering the final-state p-^{3}H system is formed from the highly correlated ^{4}He target nucleus, within which the proton and triton are in a relative ^1S state. No such initial-state correlation exists in the other reactions.

The one remaining inconsistency in Table III is the narrow width reported for this state by Parker *et al.*[5] Meyerhof[20] has analyzed this reaction in terms of the p-^{3}H phase shifts and finds fair agreement, but some difficulty with the energy scale. In our opinion the errors quoted in Ref. 5 are probably too low. The smallness of the errors arises from the "kinematic amplifier" effect discussed by Donovan.[21] The gain in accuracy as a result of this effect is, however, real only if the angles of the detectors are correspondingly well known. In the experiment under discussion any error in angle would result in an apparent change of both the energy and width of the state. A reexamination of the data in Ref. 5 would therefore be useful.

ACKNOWLEDGMENTS

Part of the computer time for analysis of the data was made available through the facilities of the Computer Science Center of the University of Maryland. One of us (H.G.P.) wishes to thank the Oak Ridge National Laboratory for financial support and warm hospitality during the summer of 1966, when this project was initiated.

[20] W. E. Meyerhof, Rev. Mod. Phys. **37**, 512 (1965).

[21] P. F. Donovan, Rev. Mod. Phys. **37**, 501 (1965).

PHYSICAL REVIEW VOLUME 178, NUMBER 4 20 FEBRUARY 1969

Nucleon Correlation Effect in the Shell-Model Description of the Deuteron*

M. A. K. Lodhi

Department of Physics, Texas Technological College, Lubbock, Texas

(Received 31 October 1968)

We have assumed that an effective central potential in place of actual N-N interaction can be used in general for finite-nucleus calculations. By introducing, however, a class of residual two-body interactions, we have studied the nucleon correlation effect in the independent-particle-model (IPM) wave functions of nuclei. As an illustrative example, this method has been applied to the deuteron. A shell-model description of the deuteron is proposed that takes proper account of the nucleon correlation and the residual potential. We have obtained an adequate agreement with the elastic electron-scattering data even for the deuteron without using the tensor force. This method should be applicable to many other nuclear problems and result in interesting predictions.

ASSUMING the nucleon-nucleon interaction as that of two free nucleons, one can make calculations to explain nuclear properties, following the work of Bruckner, Bethe, and others.[1] Since this approach is extremely difficult, some approximations have to be used to make the calculations tractable, and these cause many uncertainties. In this work we shall examine the behavior of a nuclear system with a closed shell plus two particles (or holes). Essentially, we assume nucleons moving in an averaged central field. This oversimplified field has been corrected with a residual two-body interaction which leads to the correlation of the independent-particle wave functions for the system.

The actual Hamiltonian for a nucleus of mass number A

$$H=\sum_{i=1}^{A}\left(-\frac{\hbar^2}{2m}\nabla_i^2\right)+\tfrac{1}{2}\sum_{i\neq j}^{A}V(\mathbf{r}_i-\mathbf{r}_j) \qquad (1)$$

can be written as

$$H=H_0+V_{\text{int}}, \qquad (2)$$

where

$$H_0=\sum_{i=1}^{A}\left(-\frac{\hbar^2}{2m}\nabla_i^2+U_i\right) \qquad (3)$$

and

$$V_{\text{int}}=\tfrac{1}{2}\sum_{i\neq j}^{A}V(\mathbf{r}_{ij})-\sum_{i=1}^{A}U_i, \qquad (4)$$

U_i being the central potential. Since the two-body interaction $V(\mathbf{r}_{ij})$ depends only on the relative coordinates, the choice of U_i here as the harmonic-

* Part of this work was done at the University of Wyoming during the author's visit in the summer of 1968.

[1] M. A. Preston, *Physics of the Nucleus* (Addison-Wesley Publishing Co., Reading, Mass., 1966), p. 266, and references therein; G. Breit, Proc. Nat. Acad. Sci. U.S. **46**, 746 (1960).